Title

Proteomic Analysis of the Human Cyclin-dependent Kinase Family Reveals a Novel CDK5 Complex Involved in Cell Growth and Migration*

Permalink

https://escholarship.org/uc/item/9ww5t6sf

Journal

Molecular & Cellular Proteomics, 13(11)

ISSN

1535-9476

Authors

Xu, Shuangbing

Li, Xu

Gong, Zihua

et al.

Publication Date

2014-11-01

DOI

10.1074/mcp.m113.036699

Copyright Information

Peer reviewed

Proteomic Analysis of the Human Cyclin-dependent Kinase Family Reveals a Novel CDK5 Complex Involved in Cell Growth and Migration*⑤

Shuangbing Xu‡§¶, Xu Li§¶, Zihua Gong§¶, Wenqi Wang§, Yujing Li§, Binoj Chandrasekharan Nair§, Hailong Piao§, Kunyu Yang‡, Gang Wu‡, and Junjie Chen§‖

Cyclin-dependent kinases (CDKs) are the catalytic subunits of a family of mammalian heterodimeric serine/threonine kinases that play critical roles in the control of cell-cycle progression, transcription, and neuronal functions. However, the functions, substrates, and regulation of many CDKs are poorly understood. To systematically investigate these features of CDKs, we conducted a proteomic analysis of the CDK family and identified their associated protein complexes in two different cell lines using a modified SAINT (*Significance Analysis of INT*eractome) method. The mass spectrometry data were deposited to ProteomeXchange with identifier PXD000593 and DOI 10.6019/PXD000593. We identified 753 high-confidence candidate interaction proteins (HCIPs) in HEK293T cells and 352 HCIPs in MCF10A cells. We subsequently focused on a neuron-specific CDK, CDK5, and uncovered two novel CDK5-binding partners, KIAA0528 and fibroblast growth factor (acidic) intracellular binding protein (FIBP), in non-neuronal cells. We showed that these three proteins form a stable complex, with KIAA0528 and FIBP being required for the assembly and stability of the complex. Furthermore, CDK5-, KIAA0528-, or FIBP-depleted breast cancer cells displayed impaired proliferation and decreased migration, suggesting that this complex is required for cell growth and migration in non-neural cells. Our study uncovers new aspects of CDK functions, which provide direction for further investigation of these critical protein kinases. *Molecular & Cellular Proteomics 13: 10.1074/mcp.M113.036699, 2986–3000, 2014.*

Cell division is a precisely regulated process that is mainly driven by two classes of molecules, cyclin-dependent kinases (CDKs)[1] and their activating subunits, cyclins (1–3). Cdks are the catalytic subunits of this large family of heterodimeric serine/threonine protein kinases whose best-characterized members are involved in controlling progression throughout the various cell cycle phases (2, 4, 5). According to the latest versions of human and mouse genomes, there are 20 genes encoding CDKs and five additional genes encoding a more distant group of proteins named CDK-like (CDKL1-CDKL5) kinases (2, 6). The current CDK family consists of 11 classic CDKs (CDK1–11), two newly proposed family members (CDK12 and 13), and additional proteins whose names are based on the presence of a cyclin-binding element (PFTAIRE proteins, including CDK14 and CDK15; PCTAIRE proteins, including CDK16, CDK17, and CDK18) or on a sequence relationship with the original CDKs, such as CDC2-like kinase (CDK19) or cell cycle-related kinase (CDK20).

The CDK family has been widely studied in the past two decades and implicated in control of cell-cycle progression, gene transcription, and neuronal functions, which are key events required during development, tissue homeostasis, and tumorigenesis (7, 8). In addition, because of their catalytic activities, some CDKs are considered druggable targets, and selective inhibitors for these CDKs are being developed for cancer therapy (5). Until now, the studies of some CDKs, such as those focused on CDK1, CDK2, CDK4, and CDK6, have been very extensive; however, the physiological roles of other CDKs and their activating partners remain largely unknown. Therefore, we used a modified tandem affinity purification coupled with mass spectrometry analysis (TAP-MS) approach to conduct a proteomic study of the CDK family, with a goal of understanding the regulations and functions of this critical family of protein kinases. An unexpected finding is the iden-

---

[1] The abbreviations used are: CDKs, Cyclin-dependent kinases; SAINT, Significance Analysis of INTeactome; HCIP, high-confidence candidate interacting proteins; PPI, protein-protein interaction; shRNA, short-hairpin RNA; SFB, S tag-Flag tag-SBP; GO, gene ontology.

tification of a novel CDK5-containing protein complex in non-neuronal cells.

Despite the recent recognition that many CDKs may have regulatory functions beyond cell cycle control, CDK5 remains the most unusual member of the CDK family (9). This is because unlike other CDKs, CDK5 is activated by p35 and p39, two proteins that are expressed only in the brain (10, 11). CDK5 also binds to D-type and E-type cyclins but does not display kinase activity (12). Therefore, Cdk5 is often regarded as a neuron-specific kinase, which is not involved in cell cycle control, but instead plays an essential role in neuronal development, including neuronal migration, axon guidance, and synaptic plasticity (13–16).

However, CDK5 is ubiquitously expressed. Emerging evidence indicates that CDK5 may have extraneuronal functions that comprise transcript-selective translation control, glucose-inducible insulin secretion, vascular angiogenesis, cell adhesion, migration, and wound healing (12, 17–19). Importantly, CDK5 also plays critical roles in the development and progression of many types of human cancers, which include liver cancer (20), colorectal cancer (21), pancreatic cancer (16, 22), prostate cancer (23, 24), and lung cancer (25, 26). Unfortunately, precisely how CDK5 functions outside of neuronal tissues and participates in tumorigenesis is largely unknown.

Our proteomics study of the CDK family led to the discovery of many novel CDK-associated proteins, expanded the roles of CDKs in multiple biological processes, and established comparable interaction networks in two different cell lines. Specifically for CDK5, we uncovered a novel complex that contains CDK5, a previously uncharacterized protein KIAA0528, and fibroblast growth factor (acidic) intracellular binding protein (FIBP). We provide evidence suggesting that this complex is important for regulating cell growth and migration in breast cancer cells and therefore offer a new mechanism of CDK5 function in non-neuronal tissues.

EXPERIMENTAL PROCEDURES

Plasmids and Viruses—The CDK family proteins (CDK1, CDK2, CDK3, CDK4, CDK5, CDK6, CDK7, CDK8, CDK9, CDK10, CDK13, CDK14, CDK15, CDK16, CDK17, CDK18, CDK19, CDK20, CDKL1, and CDKL4), 24 controls (RSF1, MSI1, TNK1, YES1, PTK6, LCK, TRAF6, FAF1, NDRG4, SMYD4, MXI1, TRIM16, ERCC8, BLK, FER, BMX, ZAP70, TNK2, AMOTL1, AMOTL2, ST3, STK4, TEAD2, and YAP), and KIAA0528 and FIBP plasmids were purchased from Harvard Plasmids (Harvard Medical School, Boston, MA) and Open Biosystems (Huntsville, AL). CDK11 plasmid was kindly provided by Dr. Re′gis Giet (Universite′ de Rennes I). CDK12 plasmid was kindly provided by Dr. Dalibor Blazek (University of California at San Francisco). CDKL5 plasmid was kindly provided by Dr. Marsha Rich Rosner (University of Chicago). All constructs were generated by polymerase chain reaction (PCR) and subcloned into pDONOR201 vector with use of Gateway Technology (Invitrogen, Carlsbad, CA) as the entry clones. For the TAP-MS, all entry clones were subsequently recombined into lentiviral-gateway-compatible destination vector for the expression of C-terminal SFB-tagged fusion proteins.

Gateway-compatible destination vectors with indicated SFB tag or Myc tag were also used to express various fusion proteins for the CDK5, KIAA0528, and FIBP studies. Mutations were introduced in these constructs by using the Quik-Change Site-Directed Mutagenesis Kit (Stratagene, La Jolla, CA), and all mutations were verified by DNA sequencing.

Lentivirus Packaging and Infection—All lentiviral supernatants were generated by transient transfection of HEK293T cells with packaging plasmids pSPAX2 and pMD2G (kindly provided by Dr. Zhou Song-yang, Baylor College of Medicine) and harvested 48 h after transfection. Supernatants were passed through a 0.45-μm filter and used to infect MDA-MB-231 cells with the addition of 8 μg/ml Polybrene.

Two individual pGIPZ lentiviral shRNAs targeting CDK5, KIAA0528, and FIBP, respectively, were obtained from the shRNA and ORFeome core facility at The University of Texas MD Anderson Cancer Center. The shRNA sequences were as follows:

Control shRNA: 5′-TCTCGCTTGGGCGAGAGTAAG-3′

CDK5 shRNA-1[#] (V3LHS_390938): 5′-TGAGTAGGCAGAT-CTCCCG-3′;

CDK5 shRNA-2[#] (V3LHS_390942): 5′-ATCTTTTCCAGTTT-CTCGT-3′;

KIAA0528 shRNA-1[#] (V2LHS_232289): 5′-TATTCATTAGC-TGAGTATG-3′;

KIAA0528 shRNA-2[#] (V3LHS_398207): 5′-AATTCTGTAACTTCAT-CCG-3′;

FIBP shRNA-1[#] (V3LHS_351216): 5′-TGCTGAATATTGTCCACCA-3′;

FIBP shRNA-2[#] (V3LHS_351217): 5′-TTGGTGCTGATGTCATCCA-3′;

The KIAA0528–1[#] and FIBP-1[#] shRNA resistant wild-type and mutant constructs were generated by six nucleotide substitutions and verified by DNA sequencing.

Antibodies—Anti-CDK5 antibody was purchased from Santa Cruz Biotechnology (Santa Cruz, CA). Anti-KIAA0528 antibody was purchased from Bethyl Laboratories Montgomery, TX. Anti-FIBP polyclonal antibody was purchased from Abgent. Anti-Beta-actin and anti-Flag (M2) monoclonal antibodies and anti-Flag polyclonal antibodies were obtained from Sigma-Aldrich. Anti-Myc and GAPDH monoclonal antibodies were purchased from Santa Cruz Biotechnology.

Cell Culture and Transfection—HEK293T and MCF10A cells were purchased from the American Type Culture Collection and maintained in Dulbecco modified essential medium (DMEM) supplemented with 10% fetal bovine serum at 37 °C in 5% CO_2 (v/v). MDA-MB-231 cells were kindly provided by Dr. Li Ma (MD Anderson Cancer Center). MCF10A cells were maintained in DMEM/F12 medium supplemented with 5% horse serum, 200 ng/ml epidermal growth factor, 500 ng/ml hydrocortisone, 100 ng/ml cholera toxin, and 10 μg/ml insulin at 37 °C in 5% CO_2 (v/v). All culture media contained 1% penicillin and streptomycin antibiotics. Plasmid transfection was performed with use of the polyethylenimine reagent.

Establishment of Stable Cell Lines and Affinity Purification of S-FLAG-SBP (SFB)-Tagged CDK Family Protein Complexes—HEK293T cells were transfected with plasmids encoding various SFB-tagged proteins. Stable cell lines were selected with media containing 2 μg/ml puromycin and confirmed by immunostaining and Western blotting. MCF10A cells (or MDA-MB-231 cells) were infected by lentivirus expressing tet-on inducible SFB-tagged proteins, and stable pools were selected with media containing 500 μg/ml G418 (or 2 μg/ml puromycin) and confirmed by immunostaining and Western blotting.

For affinity purification, HEK293T, MCF10A, or MDA-MB-231 cells were subjected to lysis in NETN buffer (with protease inhibitors) at 4 °C for 20 min. Crude lysates were subjected to centrifugation at 4 °C and 14,000 rpm for 20 min. Supernatants were incubated with streptavidin-conjugated beads (Amersham Biosciences) for 2 h at 4 °C. The beads were washed three times with NETN buffer, and

bounded proteins were eluted with NETN buffer containing 2 mg/ml biotin (Sigma) for 2 h at 4 °C. Elutes were incubated with S protein beads (Novagen) for 1 h. The beads were washed three times with NETN buffer and subjected to SDS-PAGE. Protein bands were excised and subjected to mass spectrometry analysis (performed by Taplin Mass Spectrometry Facility, Harvard Medical School).

Mass Spectrometry Analysis—Excised gel bands were cut into ~1 mm³ pieces. Gel pieces were then subjected to in-gel trypsin digestion (27) and dried. Samples were reconstituted in 5 μl of HPLC solvent A (2.5% acetonitrile, 0.1% formic acid). A nano-scale reverse-phase HPLC capillary column was created by packing 5 μm C18 spherical silica beads into a fused silica capillary (100-μm inner diameter x ~20-cm length) with a flame-drawn tip. After the column was equilibrated, each sample was loaded via a Famos autosampler (LC Packings, San Francisco, CA) onto the column. A gradient was formed, and peptides were eluted with increasing concentrations of solvent B (97.5% acetonitrile, 0.1% formic acid).

As peptides eluted, they were subjected to electrospray ionization and then entered into an LTQ Velos ion-trap mass spectrometer (ThermoFisher, San Jose, CA). Peptides were detected, isolated, and fragmented to produce a tandem mass spectrum of specific fragment ions for each peptide. All the default parameters were used. Peptide sequences (and hence protein identity) were determined by matching the acquired fragmentation pattern with protein databases by the software program, SEQUEST (ver. 28) (ThermoFisher). Enzyme specificity was set to partially tryptic with two missed cleavages. Modifications included carboxyamidomethyl (cysteines, fixed) and oxidation (methionine, variable). Mass tolerance was set to 2.0 for precursor ions and to 1.0 for fragment ions. Because we used HEK293T and MCF10A cells, the database searched was the Human IPI databases version 3.6. The number of entries in the database was 160,900, which included both the target (forward) and the decoy (reversed) human sequences. Spectral matches were filtered to contain less than 1% FDR at the peptide level based on the target-decoy method (28). Finally, only tryptic matches were reported, and spectral matches were manually examined. When peptides matched to multiple proteins, the peptide was assigned so that only the most logical protein was included (Occam's razor). This same principle was used for isoforms when present in the database. The longest isoform was reported as the match. The mass spectrometry proteomics data have been deposited to the ProteomeXchange Consortium (http://proteomecentral.proteomexchange.org) via the PRIDE partner repository with the data set identifier PXD000593 and DOI 10.6019/PXD000593 (29–31). supplemental Table S1 contains the lists of the proteins identified during these analyses. supplemental Table S2 contains the lists of the peptides identified and during these analyses.

Data Analysis and Bioinformatics Analysis—To apply SAINT algorithms, we first gathered information about baits and preys including the spectra counts, prey protein length, and assignment of control baits. We reorganized the data to the format compatible to the SAINT program and used two-pool analysis, which recognizes the control group as a separate pool. We did not remove outlier data points. However, during the data analysis, we temporarily removed the bait self-identification in the identification list before applying the SAINT algorithms, and added it back after the data filtration. The statistics used to assess accuracy and significance of measurements was referred to the SAINT algorithms, where SS (SAINT score) > 0.80 was taken as the threshold required for the data quantification, as indicated by the SAINT method (32).

For overall interactomes generated by Cytoscape (33, 34), we analyzed the network and created custom styles, then applied *y*Files organic layout with minor adjustments when necessary. For the individual CDK interactomes generated by Cytoscape, we used unweighted force directed distributions with minor adjustments when

necessary. The reported interactions (orange lines) were performed with literature-based search provided by BioGrid (35) and other databases when necessary.

The heatmap for the hierarchical clustering was generated by MEV_4.8.1 Heatmap Builder software. For the prey-bait heat-map, we used HCL clustering based on Pearson correlation with average linkage clustering and set the color lower limit to 0, midpoint value to 10.0, and upper limit to 20.0.

The Gene-Ontology annotations with *p* values were performed based on the Knowledge Base provided by Ingenuity pathway software (Ingenuity Systems, www.ingenuity.com), which contains findings and annotations from multiple sources including the Gene Ontology database. We used -log (*p* value) of individual functions to make GO annotation heatmaps. In these GO-heatmaps, we arranged the baits in alphabetical order and did not cluster them. We used a rainbow scheme and set the color lower limit to 1, midpoint value to 2.5, and upper limit to 5.0.

Western Blotting and Immunoprecipitation—Cells were lysed in NETN buffer (20 mM Tris-HCl, pH 8.0, 100 mM NaCl, 1 mM EDTA, and 0.5% Nonidet P-40), and the clarified lysates were resolved by SDS-PAGE and transferred to PVDF membranes for Western blotting. Alternatively, the clarified supernatants were first incubated with S-protein beads (Novagen, Madison, WI) for 2 h, and the precipitates were washed five times with NETN buffer. To investigate the interaction between CDK5 and KIAA0528 or FIBP at the endogenous level, the clarified supernatants were first incubated with anti-CDK5 or KIAA0528 for 2 h at 4 °C. Protein A/G-agaroses were then added overnight, and the precipitates were washed five times with NETN buffer and analyzed by Western blotting.

Cell Proliferation Analysis—This assay was performed as described previously (36). Briefly, CDK5-, KIAA0528-, or FIBP-deficient, reconstituted, or control MDA-MB-231 cells were seeded at low density (1.6 × 10⁴ cells/6 well plate). Cell numbers were quantified every day by digesting cells into suspension using trypsin/EDTA and resuspending in a given volume of fresh medium. The data presented represent the mean of all measured points ±S.E. (*n* = 3).

Soft-Agar Colony Assay—The soft-agar colony assay was performed essentially as described previously (37). Briefly, MDA-MB-231 cells (2.5 × 10³) were added to 1.5 ml of growth medium with 0.33% agar and layered onto beds of 0.5% agar (2 ml) in six-well plates. Viable colonies were scored after 3 weeks of incubation, and the quantified data were presented from three independent experiments.

Wound Healing Assay—This assay was performed as described previously (38). Briefly, Confluent MDA-MB-231 cells were scratched with 200 μl pipette tips, washed twice with PBS, and then refreshed with appropriate medium. Images were captured 22 h later with use of a microscope.

Transwell Migration Assays—This assay was performed as described previously (39). Briefly, 5.0 × 10⁴ MDA-MB-231 cells in 200 μl of serum-free DMEM were added to the cell culture inserts with an 8-μm Pore Polycarbonate Membrane (Corning, NY, USA). DMEM conditioned medium containing 10% FBS was added to the bottom chamber. After 22 h of incubation, the cells on the lower surface of the chamber were fixed, stained, and then examined with use of a microscope. The numbers of migrated cells in three random optical fields from triplicate filters were averaged.

RESULTS

Proteomic Analysis of the Human CDK Family—To establish the protein-protein interaction (PPI) network of the human CDK family, we conducted proteomic analyses with use of tandem affinity purification followed by mass spectrometry (TAP-MS) in two different cell lines: SV40 large T antigen
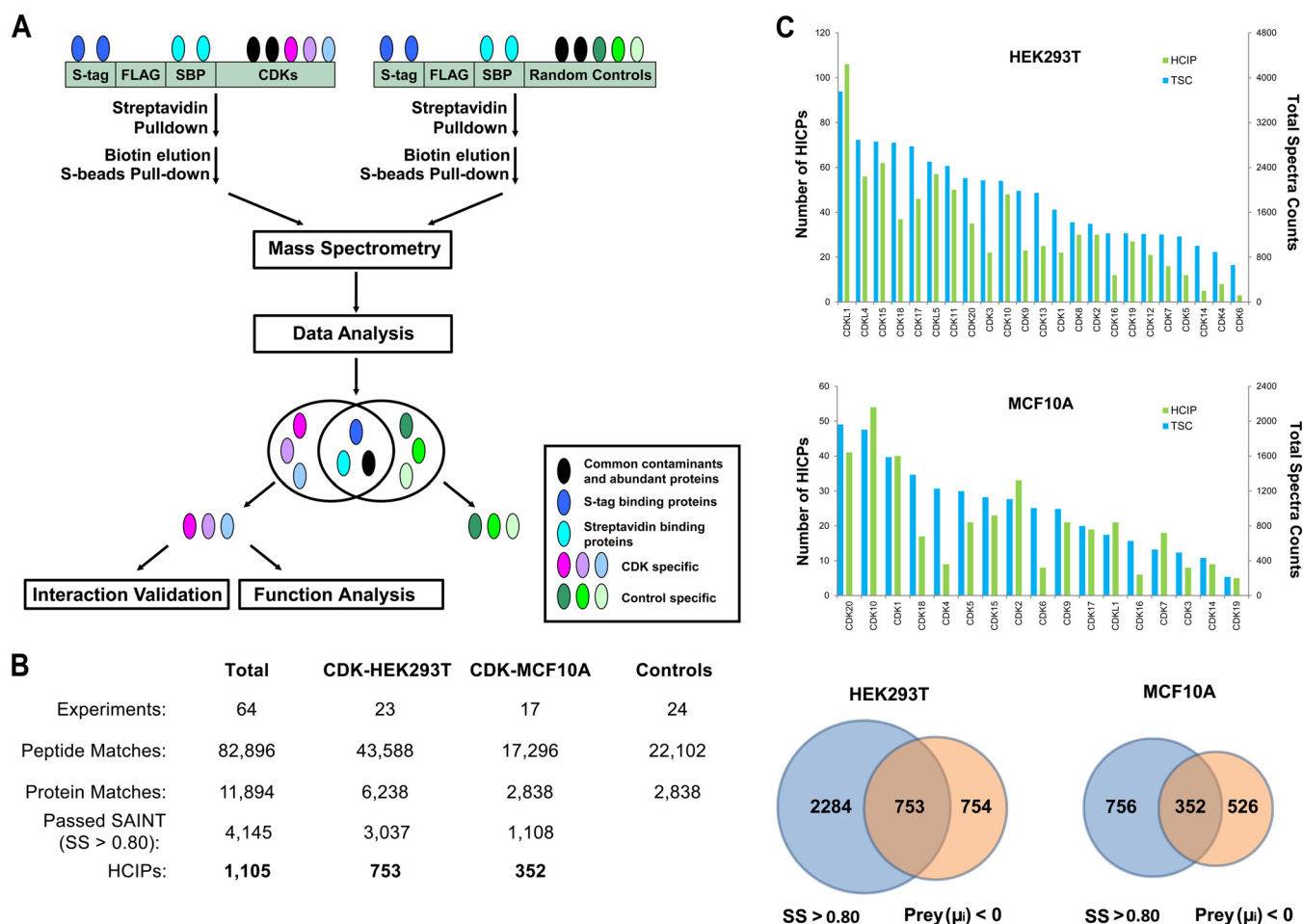
FIG. 1. **Proteomic analysis of the human CDK family proteins.** *A*, Major steps involved in the tandem affinity purification-mass spectrometry analysis of the human CDK family. *B*, The total peptide and protein numbers obtained from mass spectrometry analysis are listed. The probability threshold SS> 0.80 was used as the cutoff to identify HICPs, as suggested by the SAINT method. We also applied an additional filtration by using the prey information in 24 control purifications to remove the nonspecific or common binding proteins ($\mu_i < 0$). The intersection of SS > 0.8 and $\mu_i < 0$ were considered as HCIPs. *C*, The total spectral counts (TSC; *blue*) and corresponding number of HICPs (*green*) for each CDK bait protein are shown together.

transformed human embryonic kidney 293 (HEK293T) cells and immortalized, nontransformed human breast epithelial MCF10A cells. Briefly, HEK293T or MCF10A derivative cell lines stably expressing each of these SFB triple-tagged CDKs were established. Western blotting and immunostaining were performed to validate the correct protein expression and cellular localization for each cell line (data not shown). After two rounds of affinity purifications, proteins in the final eluate were identified by LC-MS/MS analysis (Fig. 1*A*). The complete protein-identification and peptide-identification lists are shown in supplemental Tables S1 and S2. Of a total of 25 human CDKs and CDK-like kinases, we successfully conducted TAP-MS analysis for 23 CDKs in HEK293T cells (lack of CDKL2 and CDKL3 because of low expression) and 17 CDKs in MCF10A cells (lack of CDK11, CDK12, CDK13, and CDKL5 because of no expression, and lack of CDK8, CDKL2, CDKL3, and CDKL4 because of low expression).

For the evaluation of potential CDK-interacting proteins, raw data from the mass spectrometry analysis were subjected to the modified SAINT algorithm (Significance *Anal*ysis of *INT*eractome) (40, 41), an unbiased filtration methodology for identification of high-confidence candidate interacting proteins (HCIPs) (Fig. 1*B*), which we have used recently for analysis of the human Hippo pathway (42). The spectra counts from the CDK group and control group proteins were assembled as a matrix for all of the bait and prey proteins. In total, 11,894 protein matches were identified in 64 experiments, with 23 CDKs purified from HEK293T cells, 17 CDKs purified from MCF10A cells, and 24 control SFB-tagged unrelated protein purifications in HEK293T or MCF10A cells (18 in HEK293T cells and six in MCF10A cells).

According to the SAINT algorithms, 10,000 simulation runs were performed for Gibbs sampling. The total spectra count

(TSC) was fixed for each bait, and these spectra counts were assembled as a pool of all of the bait spectra counts. Then we randomly drew spectra from the pool and randomly assigned them to the baits until the number of spectra reached the number in the real data. We simulated 50,000 such runs to get the distribution of SAINT probability scores by random chance. The separation of positive and negative distributions was considered but not for the impact of extremely high-count interactions on the scoring of low-count interactions or for division of spectra counts by the total spectra counts of each purification. We have evaluated the use of different SAINT scores as cut-offs in our data analysis by assessing whether the HCIPs generated by different cut-offs would overlap significantly with the BioGrid (35) and CRAPome (43) to get respectively the percentages of the "true positive" and "potential false positive" results. We found that using any cut-off score between 0.6 and 0.95 did not significantly change the quality of HCIPs (supplemental Fig. S1A). There-fore, we kept interactions with probability scores higher than 0.8 for further analysis, similar to that suggested by the orig-inal SAINT paper (44). By performing analysis of overlapping with CRAPome, we also demonstrated that our control data-set comprising unrelated protein purifications serves as better controls than mock purifications using vector alone (supple-mental Fig. S1B). A total of 4145 interactions passed this first filtration: 3037 in the HEK293T group and 1108 in the MCF10A group (Fig. 1B).

We used the semi-supervised mixture model to further elim-inate common contaminates and abundant proteins. The false-positive score μ_i of individual preys, which is a param-eter estimated by the Poisson mixture model using the SAINT algorithm, were also used to calculate the probability of abun-dant/nonspecific baits frequently shown in the interactions. It represents the difference of the estimated prey abundance between the negative control group and the entire group (sample + control). $\mu_i \geq 0$ indicates the abundance of a given prey in the negative control group is equal to or higher than that in the entire group, which means that this particular prey may not be specific. We eliminated any prey with $\mu_i \geq 0$. Common contaminants and abundant proteins were removed at this step. A total of 2385 interactions passed this filtration: 1507 in the HEK293T group and 878 in the MCF10A group. We combined the interactions that passed both filtrations, which is the intersection of SS > 0.8 and $\mu_i < 0$. Total 1105 interactions were designated as HCIPs: 753 were in HEK293T cells and 352 were in MCF10A cells (Fig. 1B and supplemental Table S3), which represents 603 unique preys. The HCIPs for each bait protein identified here (Fig. 1C) were considered CDK interactomes in HEK293T and MCF10A cells (supple-mental Fig. S2). Interestingly, 57 bait-prey interactions were shown in both HEK293T and MCF10A cells (supplemental Fig. S1); 89 preys appeared in both cell lines, although the baits with which they interacted could be different, which may be

because of the fact that some preys may have preference for different CDKs in two different cell lines.

Overview of the PPI Network of Human CDK Family—To understand the relationship among human CDK family pro-teins, we analyzed the networks using Cytoscape (34), then used *y*Files organic layout (*y*Works®) to cluster the baits and preys. We first generated interactomes for the whole CDK family in HEK293T cells (Fig. 2A) and MCF10A cells (Fig. 2B). By merging them into a unified network (Fig. 2C), we were able to achieve better clustering and obtained several CDK sub-networks. These networks include previously known CDK1–2-3 network (Fig. 3C), CDK8–19 network (supplemen-tal Fig. S2A), newly identified CDK11–12-13 network (supple-mental Fig. S2B), CDK17–18 network (supplemental Fig. S2C), and CDK10–15-20 network (supplemental Fig. S2D).

We have also carried out an unbiased hierarchical cluster-ing to confirm these bait-prey clusters in two different cell lines (supplemental Fig. S3A), and observed all these clusters (supplemental Fig. S3B). For example, CDK8/CDK19 sub-network (supplemental Fig. S2A, cluster 3 in Supplemental Fig. S3B) revealed the previously reported crosstalk between CDK8 and CDK19, both of which are involved in RNA polym-erase II (pol II) transcription as components of the Mediator complex (45). Indeed, we identified many other subunits of the Mediator complex in this cluster. The other example is the CDK11/CDK12/CDK13 sub-network (supplemental Fig. S2B, cluster 4 in supplemental Fig. S3B). These proteins have been proposed to regulate alternative splicing in RNA processing (46, 47). Interestingly, the clustered preys consisted of two RNA binding proteins RBM15 and RBM25, which function in efficient mRNA export and alternative pre-mRNA splicing (48, 49), suggesting that CDK11, CDK12, and CDK13 may have redundant functions in controlling RNA splicing via regulating these RNA binding proteins. Our results suggested that CDK proteins in the same clusters are likely to function together in the same or similar pathways.

To illustrate the diversity and similarity of prey-bait interac-tions in two different cell lines, we computed the overlaps between the HCIPs obtained in two different cell lines (Fig. 3A). To our surprise, only a few interactions were shown in both cell lines. This could be caused by multiple reasons. The technical reason could be that the purifications in MCF10A cells recovered fewer peptides in comparison with those per-formed in HEK293T cells and therefore some relatively weak interactions may not be detectable in MCF10A cells. This was caused by the lower expression of baits in MCF10A cells. To test whether this is the case, we compared the overlap of interaction and peptides between two cell lines using two, three, five, and eight peptides as cut-offs (Fig. 3B). The HCIPs identified in MCF10A significantly merged with those in HEK293T with the increasing of peptide numbers, indicating that some HCIPs recovered in HEK293T cells may be missing in MCF10A cells because their low peptide counts. Of course, some of these differences could be caused by biological
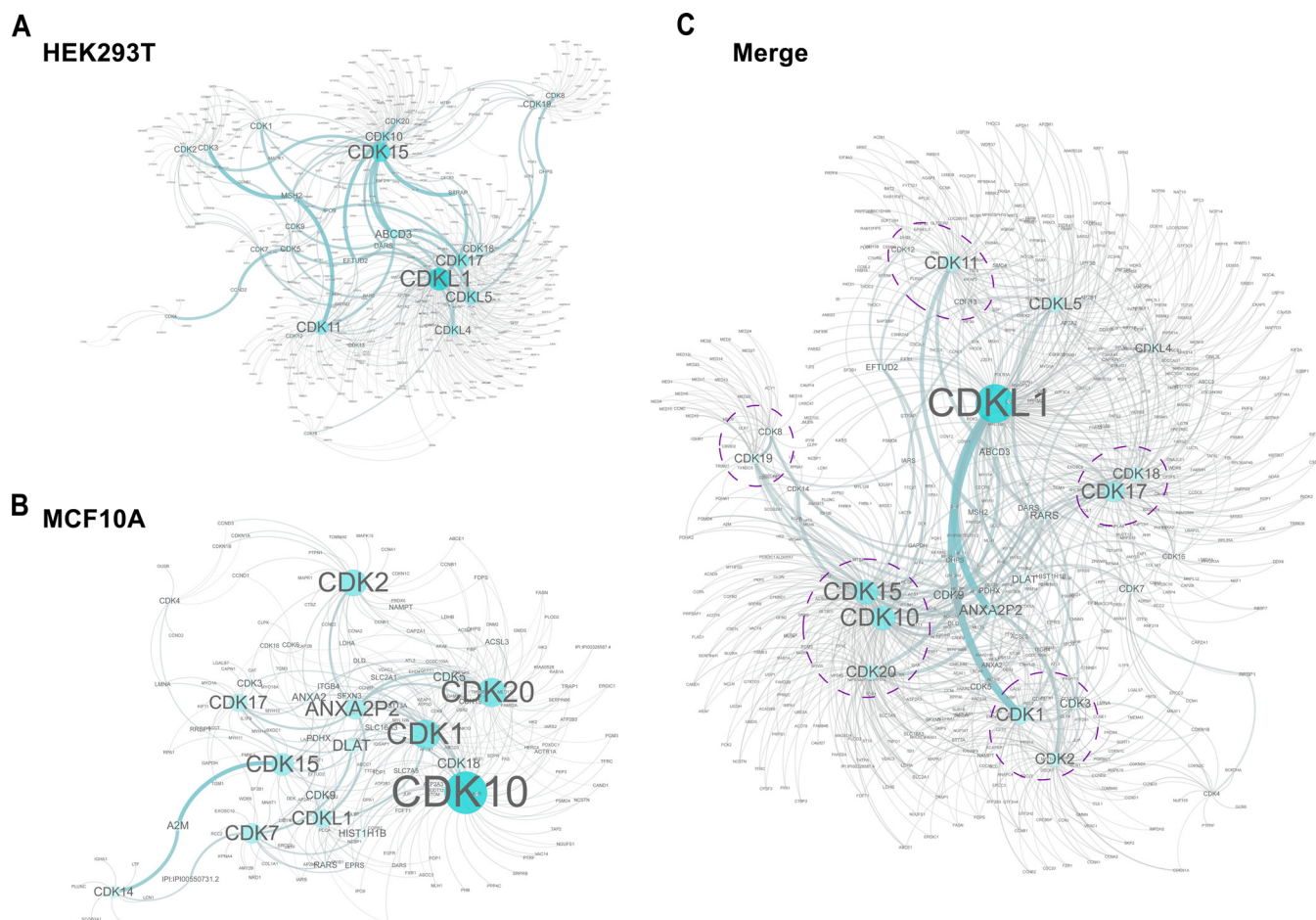
FIG. 2. **Interactomes of the human CDK family identified in HEK293T and MCF10A cells.** The human CDK interactomes, which include *A*, 753 HCIPs identified in HEK293T cells, *B*, 352 in MCF10A cells, and *C*, merged networks were generated with use of Cytoscape software. The networks were analyzed and generated with customized styles, then used *y*Files organic layout (*y*Works®) to cluster the baits and preys. Five CDK sub-family clusters were circled with dashed lines in *C*.

reasons, for example, the endogenous prey protein expression levels may vary significantly in different tissue or cell lines.

To get further insight into the difference between cell lines, we established the CDK1–2-3 sub-network (Fig. 3*C*). As shown in Fig. 3*C* and clustered in supplemental Fig. S3*C*, CDK1, CDK2, and CDK3 shared the same preys CCNA1, CCNA2, and SKP2 in HEK293T cells (clusters 1 and 2). CDK1 and CDK2 shared the same preys CCNB1 and CCNB2 in both cells (clusters 2 and 5). Interestingly, we observed cell type preference of the cyclins, for example, CDK2 binds to CCNB1/2 and CCNE1/2 in both cell lines, but CCNA1/2, CCNH, and CCNJ only in HEK293T cells, and CCND1/3 only in MCF10A cells (Fig. 3*C*). These could be caused by some intrinsic differences in these two cell lines, for example, the expression levels of these preys, the proliferation status of these cell lines, and/or the presence of SV40 T antigen in HEK293T cells.

To characterize the CDK family and its associated proteins in the context of biological processes, we carried out a Gene Ontology (GO) analysis to identify the GO process for each bait-associated HCIP (supplemental Fig. S5). GO process analysis linked the CDK family to a wide variety of cellular functions primarily focusing on the cell cycle, RNA posttranscriptional modification, cellular development, cell death and survival, cellular growth and proliferation, as well as DNA replication, recombination, and repair, all of which are fundamental missions carried out by the CDK family. These major cellular functions contribute to the systematic roles of the human CDK family in embryonic development, connective tissue development and function, and tissue morphology, which clearly are linked to the known functions of the CDK family in organ development and homeostasis. The disease and disorder GO analysis linked the human CDK family to cancer, hematological disease, developmental disorders, and metabolic disease, which have already been studied extensively for human CDKs.

CDK5 Interactome Validation Reveals a Stable Protein Complex that Consists of CDK5, KIAA0528, and FIBP—To verify our proteomic data, all of the HCIPs were searched

FIG. 3. **Comparison of the interactomes in HEK293T and MCF10A cells.** *A*, HCIPs shown in both cell lines. *B*, The percentages and numbers of HCIPs in each cell lines and their overlaps. Red: in HEK293T cells; blue: in MCF10A cells; purple: in both cells. *C*, An example of CDK1–2–3 sub-network in two cell lines. Red: in HEK293T cells; blue: in MCF10A cells; purple: in both cells. The orange line indicates the reported protein-protein interaction. The gray line indicates the newly identified interaction from the current study.

against various PPI databases, which included BioGrid, STRING, BIND, DIP, and HPRD. A total of 136 interactions among the 753 HCIPs (18.1%) in HEK293T cells and 57 interactions among the 352 HCIPs (16.2%) in MCF10A cells have been previously reported (supplemental Table S3). However, given that there is no interaction record for many CDKs such as CDK10, CDK15, CDK16, CDK17, CDK18, CDKL1, CDKL4, and CDKL5 in these databases, the positive rate is reasonable and credible.

There is a substantial difference between the PPIs identified in the two cell lines. For example, 16 of 22 preys (72.7%) in CDK1 and 27 of 30 preys (90%) in CDK2 identified in HEK293T cells have been reported previously (supplemental Table S3). In contrast, only five of 39 preys (12.8%) in CDK1 and 17 of 33 preys (51.5%) in CDK2 identified in MCF10A cells have been validated (supplemental Table S3). This dif-

ference likely reflects the fact that many previous studies were performed in transformed or cancer cell lines. Our data indicate that proteomics analysis in MCF10A, albeit challenging, may be necessary, because it can help us uncover potential novel functions of CDKs in "normal" cells.

To further validate our proteomics data, we decided to perform an in-depth study of the CDK5 interactome. In this interactome, we identified many previously reported CDK5-associated proteins, including Cables1 (50), Cables2 (51), CCND2 (52), and CCNI (53) (Fig. 4*A* and 4*B*). Importantly, we repeatedly uncovered KIAA0528 and FIBP as major CDK5-associated proteins in two different cell lines (Fig. 4*A* and 4*B*). To confirm that KIAA0528 and FIBP exist in the same complex as CDK5, we performed reversal TAP-MS analysis by using SFB-tagged KIAA0528 or FIBP as the bait protein and were excited to recover peptides that corresponded to the other
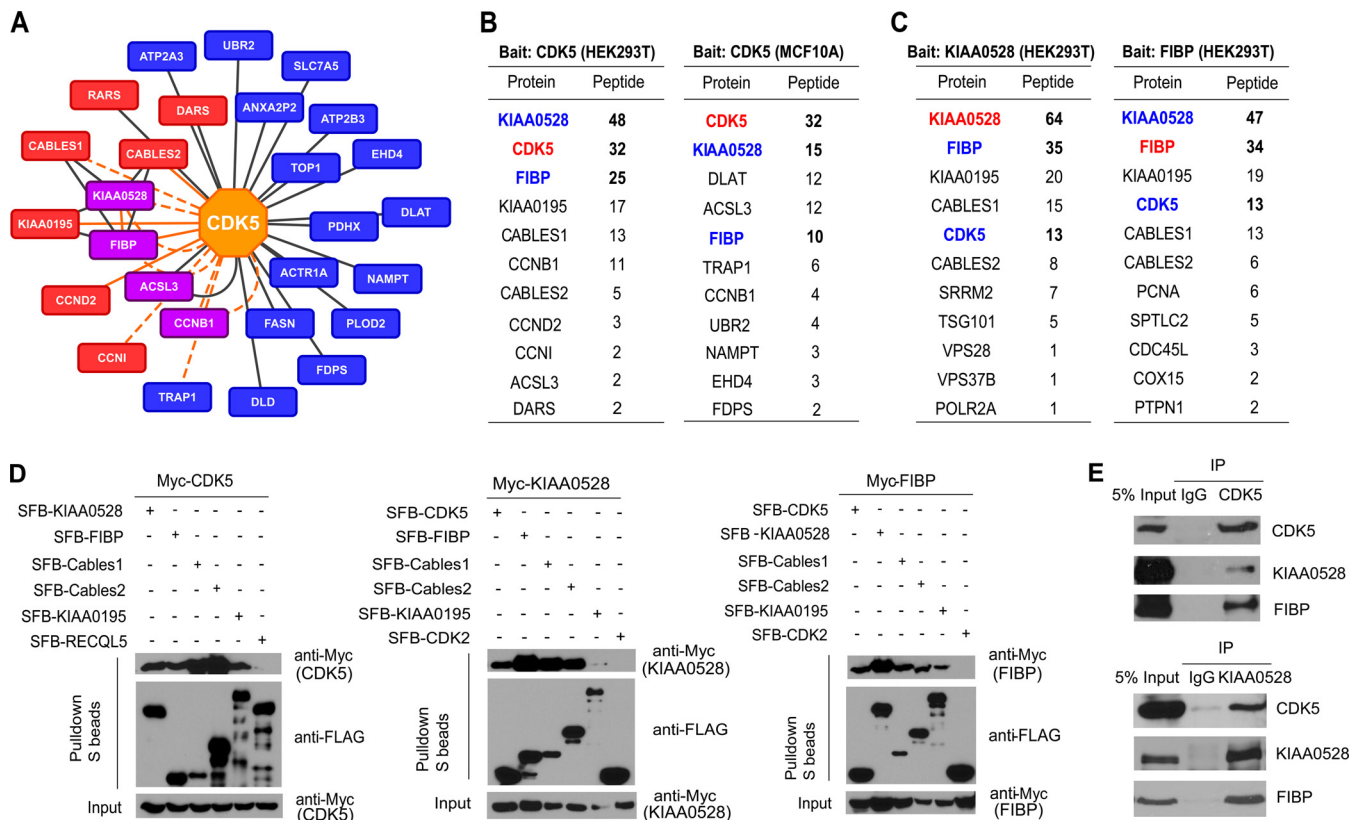
A

B

Bait: CDK5 (HEK293T)		Bait: CDK5 (MCF10A)	
Protein	Peptide	Protein	Peptide
KIAA0528	48	CDK5	32
CDK5	32	KIAA0528	15
FIBP	25	DLAT	12
KIAA0195	17	ACSL3	12
CABLES1	13	FIBP	10
CCNB1	11	TRAP1	6
CABLES2	5	CCNB1	4
CCND2	3	UBR2	4
CCNI	2	NAMPT	3
ACSL3	2	EHD4	3
DARS	2	FDPS	2

C

Bait: KIAA0528 (HEK293T)		Bait: FIBP (HEK293T)	
Protein	Peptide	Protein	Peptide
KIAA0528	64	KIAA0528	47
FIBP	35	FIBP	34
KIAA0195	20	KIAA0195	19
CABLES1	15	CDK5	13
CDK5	13	CABLES1	13
CABLES2	8	CABLES2	6
SRRM2	7	PCNA	6
TSG101	5	SPTLC2	5
VPS28	1	CDC45L	3
VPS37B	1	COX15	2
POLR2A	1	PTPN1	2

D

E

FIG. 4. **Identification of KIAA0528 and FIBP as CDK5-associated proteins in HEK293T and MCF10A cells.** *A*, Major CDK5-interacting proteins in two different cell lines. Red: in HEK293T cells; blue: in MCF10A cells; purple: in both cells. The solid orange line indicates the reported protein-protein interaction confirmed by low-throughput methods (*e.g.* Co-IPs). The dashed orange line indicates that this interaction was reported by other high-throughput studies. The solid gray line indicates the newly identified interaction from the current study. *B*, Mass spectrometry analysis uncovered multiple CDK5-associated proteins in HEK293T and MCF10A cells. The number of peptides for each protein identified by mass spectrometry analysis was listed. Letters in red indicate the bait proteins. *C*, KIAA0528- and FIBP-associated proteins were also revealed by TAP-MS analysis in HEK293T cells. The number of peptides for each protein identified by mass spectrometry analysis was listed. Letters in red indicate the bait proteins. *D*, CDK5 associates with KIAA0528 and FIBP. Myc-tagged CDK5, KIAA0528, or FIBP was co-expressed with the indicated SFB-tagged proteins in HEK293T cells. Pulldown experiments were carried out with S protein beads, and immunoblotting was performed with anti-Myc and Flag antibodies. SFB-RECQL5 and CDK2 were included as negative controls for the co-IP experiments. *E*, Endogenous interaction between CDK5, KIAA0528, and FIBP. Immunoprecipitation was performed with use of IgG, anti-CDK5, or anti-KIAA0528 antibodies and was analyzed by Western blotting using indicated antibodies.

two proteins (Fig. 4*C*). These data suggest that CDK5, KIAA0528, and FIBP likely form a stable complex *in vivo*.

KIAA0528 (C2 calcium-dependent domain containing 5, also known as C2CD5, CDP138) was originally identified as a substrate for Akt2 (54), which was proposed to be required for optimal insulin-stimulated glucose transport, GLUT4 translocation, and fusion of GLUT4 vesicles with the PM in live adipocytes (54). However, this function of KIAA0528 is still being debated because a recent study reported that CDP138 (also known as KIAA0528, C2CD5) is not involved in GLUT4 translocation (55). FIBP is an intracellular protein that binds selectively to acidic fibroblast growth factor (aFGF) and may be involved in the mitogenic action of aFGF (56, 57). In addition, it is reported that FIBP inhibits estradiol production in regressing subordinate follicles (58). However, no further studies of the structures or other biological functions of KIAA0528 and FIBP were conducted, especially in tumorigenesis.

To verify the interactions among CDK5, KIAA0528, and FIBP, we performed coimmunoprecipitation experiments. We used SFB-Cables1 (positive control), SFB-Cables2 (positive control), and SFB-RECQL5 (negative control) and found that KIAA0528, FIBP, and KIAA0195 could specifically coimmuno-precipitate Myc-CDK5 (Fig. 4*D*). Similarly, by using SFB-CDK2 as a negative control, we also verified the specific binding of KIAA0528 and FIBP with CDK5 (Fig. 4*D*). The binding of KIAA0528 and FIBP is very strong, and of note, we found that in HEK293T cells, CDK5, KIAA0528, and FIBP can also bind to three other proteins: KIAA0195, Cables1, and Cables2. However, KIAA0195, Cables1, and Cables2 did not appear in the CDK5 complex isolated from MCF10A cells, indicating that the CDK5/KIAA0528/FIBP complex is the major complex and generally exists in cells from different origins. Moreover, endogenous CDK5, KIAA0528, and FIBP also associated with each other (Fig. 4*E*). Together, these data agree
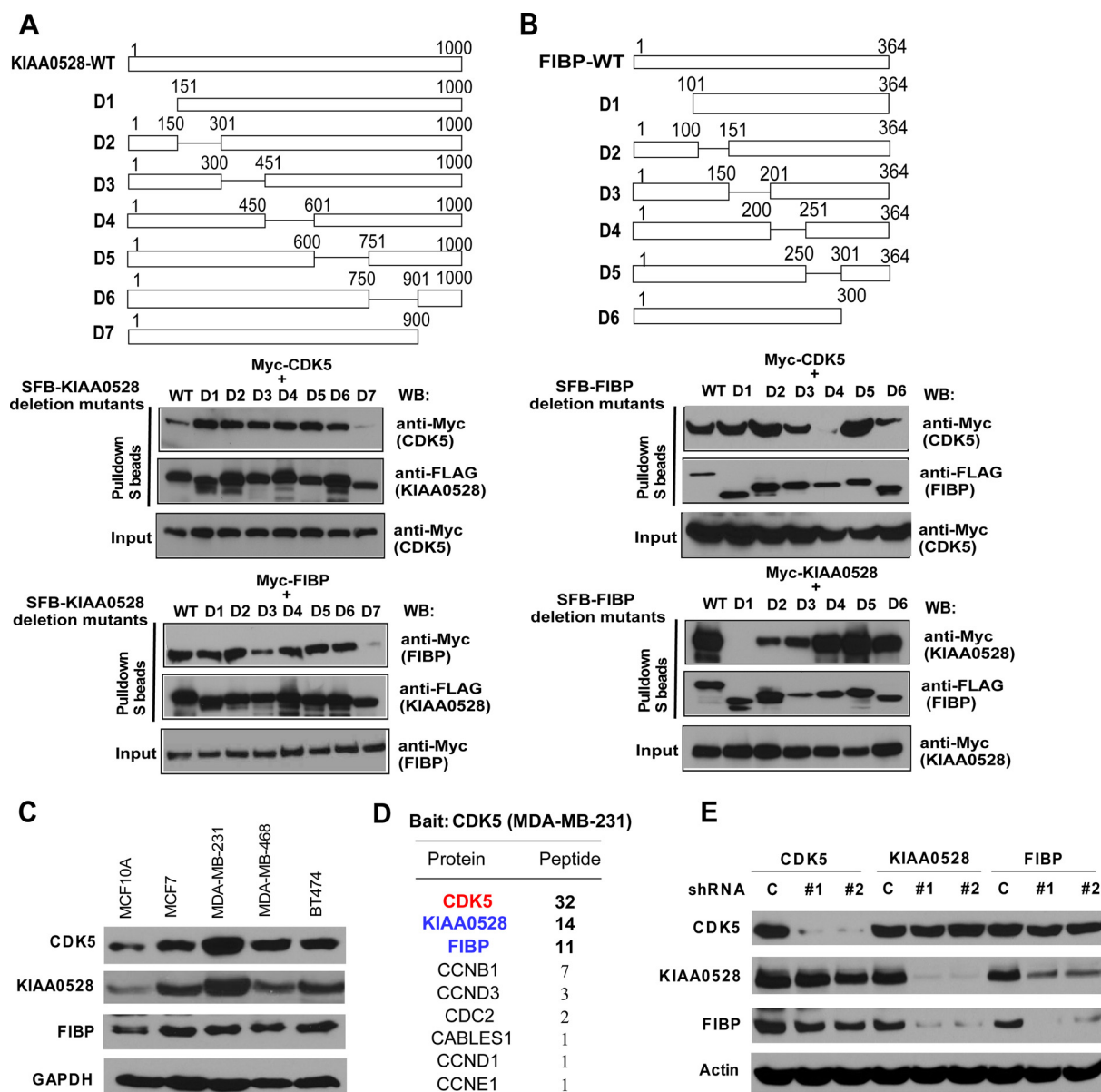
FIG. 5. **KIAA0528 and FIBP stabilize each other in the cell.** *A*, The very C-terminal region of KIAA0528 is required for its binding to CDK5 and FIBP. *Upper:* Schematic presentation of wild-type and deletion mutants of KIAA0528 used in this study. *Lower:* Mapping of the corresponding regions required for the KIAA0528/CDK5 or KIAA0528/FIBP interaction. Immunoprecipitation reactions were performed with use of S-protein beads and then subjected to Western blot analyses by using antibodies as indicated. *B*, The N-terminal region of FIBP is required for its interaction with KIAA0528. *Upper:* Schematic presentation of wild-type and deletion mutants of FIBP used in this study. *Lower:* Mapping of the corresponding regions required for the FIBP/CDK5 or FIBP/KIAA0528 interaction. Immunoprecipitation reactions were performed by using S-protein beads and then subjected to Western blot analyses by using antibodies as indicated. *C*, Immunoblots showing levels of CDK5, KIAA0528, and FIBP in lysates prepared from five different breast cell lines. Cells were harvested and cell lysates were blotted with indicated antibodies. *D*, TAP-MS analysis revealed CDK5-associated proteins in MDA-MB-231 cells. The number of peptides for each protein identified by mass spectrometry analysis was listed. Letters in red indicate the bait proteins. *E*, KIAA0528 and FIBP stabilize each other in MDA-MB-231 cells. Two different lentiviral shRNAs were used to infect MDA-MB-231 cells, and stable knockdown pools were generated. These stable cells were harvested and cell lysates were immunoblotted with antibodies as indicated.

with the TAP-MS data and support the notion that CDK5, KIAA0528, and FIBP form a complex in cells.

Mapping the Interaction Domains of CDK5, KIAA0528, and FIBP—Next, we attempted to determine the regions responsible for the interactions between CDK5, KIAA0528, and FIBP.

A series of deletion mutants of KIAA0528 or FIBP were generated (Fig. 5*A* and 5*B*), and co-IP experiments were performed to map the domains required for their interactions with the two other proteins. We showed that the very C terminus of KIAA0528 (residues 901–1000) is responsible for its binding to

CDK5 and FIBP (Fig. 5*A*). In contrast, residues 201–250 of FIBP were required for its binding to CDK5, whereas the N terminus (residues 1–100) of FIBP is essential for its binding to KIAA0528 (Fig. 5*B*). Together, these results suggest that FIBP interacts with KIAA0528 and CDK5 via various regions and may serve as a bridging protein between CDK5 and KIAA0528.

KIAA0528 Controls the Stability of FIBP and Vice Versa— CDK5, KIAA0528, and FIBP form a complex in MCF10A cells, which is an immortalized, *nontransformed* human mammary epithelial *cell line*. The protein levels of CDK5, KIAA0528, and FIBP are generally higher in breast cancer cell lines than they are in MCF10A cells (Fig. 5*C*). The expression of CDK5 and KIAA0528 in MDA-MB-231 cells are the highest among the few cell lines we checked (Fig. 5*C*). As expected, we performed tandem affinity purification (TAP) using MDA-MB-231 cells stably expressing SFB-CDK5 and further verified that CDK5 associates with KIAA0528 and FIBP in these cells (Fig. 5*D*).

The absence of a critical subunit of a multicomponent protein complex often destabilizes the complex (59). Therefore, we depleted each subunit with use of two different shRNAs and examined the stability of the others. As shown in Fig. 5*E*, depletion of CDK5 did not lead to any significant change in KIAA0528 or FIBP protein level; however, depletion of KIAA0528 resulted in a dramatic decrease in FIBP, but not CDK5, protein level. Likewise, knockdown FIBP reduced expression of KIAA0528 but not of CDK5. These results suggest that KIAA0528 may help to stabilize FIBP and vice versa in the cell. CDK5 had no effect on the expression of KIAA0528 or FIBP, indicating that CDK5 may not be limited to the KIAA0528/FIBP complex and may exist in other complexes.

*CDK5, KIAA0528, and FIBP Participate in Breast Cancer Cell Growth and Migration—*Given that prostate and pancreatic cancer cells deficient in CDK5 display impaired cell growth and decreased migration (16, 23), we examined whether loss of CDK5, KIAA0528, or FIBP would result in similar phenotypes in MDA-MB-231 cells, which exhibit highly aggressive and metastatic potential. As shown in Fig. 6*A*, we first generated two CDK5, KIAA0528, or FIBP stable knockdown MDA-MB-231 derivative cell lines. As expected, knockdown of CDK5 dramatically inhibited cell proliferation when compared with that of control cells (Fig. 6*B*). Interestingly, we also found that depletion of KIAA0528 or FIBP impaired cell proliferation (Fig. 6*B*). Moreover, decreased proliferation of CDK5-, KIAA0528-, or FIBP-depleted cells was accompanied by the decreased ability of these cells to form anchorage-independent colonies in soft agar (Fig. 6*C*), indicating that KIAA0528 and FIBP contribute to cell growth, as CDK5 does.

Using the wound-healing assay, we showed that CDK5 knockdown cells migrated slower than did control shRNA-transfected MDA-MB-231 cells (Fig. 6*D*). Similarly, KIAA0528 or FIBP depletion also suppressed cell migration (Fig. 6*D*). These phenotypes were further validated by Transwell assays.

As shown in Fig. 6*E*, knockdown CDK5, KIAA0528, or FIBP dramatically inhibited cell migration, suggesting that this CDK5 complex also participates in cell migration.

To confirm that the observed cell growth and migration defects are indeed a consequence of KIAA0528 or FIBP deficiency and to further explore whether interaction between KIAA0528 and FIBP is required for these processes, we reconstituted KIAA0528 or FIBP knockdown cells with use of retroviral KIAA0528 or FIBP expression vectors (Fig. 7*A*). Restoring wild-type, but not the C-terminal deletion mutant, of KIAA0528 expression rescued the decreased level of FIBP in the cell (Fig. 7*A*). Likewise, restoring wild-type, but not the N-terminal deletion mutant, of FIBP reestablished KIAA0528 expression in these cells (Fig. 7*A*). As shown in Fig. 7*B* and 7*C*, whereas expression of shRNA-resistant wild-type KIAA0528 or FIBP rescued defects in cell growth and cell migration in KIAA0528 or FIBP knockdown cells, reconstitution with the C-terminal deletion mutant of KIAA0528 or the N-terminal deletion mutant of FIBP failed to do so. Taken together, these results suggest that KIAA0528 and FIBP stabilize each other and that this complex is required for normal cell growth and migration.

DISCUSSION

In this study, we conducted a proteomic analysis and revealed the extensive PPI network of the CDK family. Based on this study, we uncovered a total of 1105 HCIPs, which greatly broadens our current understanding of the functions of the CDK family and provides directions for future investigation. We merged the data obtained from two different cell lines and generated a more complete CDK family interactomes (Fig. 2). We identified several previously unrecognized CDK sub-networks such as CDK11/12/13, CDK10/15/20, and CDK17/18 networks (Fig. 2 and supplemental Figs. S2 and S3). We also compared the differences between the two cell lines (Fig. 3) and found CDKs bind to very different groups of proteins. The difference in HCIPs obtained from these two cell lines could be caused by multiple reasons, including the technical and biological reasons discussed above in the Result section. The biological differences could be more interesting and may prompt further investigation. The endogenous prey protein expression levels can be very different in different tissues or cell lines. Although CABLES1/2 and KIAA0195 are previously reported CDK5-interacting proteins (Fig. 4*A*), according to protein atlas database, their RNAs and proteins are undetectable in breast tissues, but relatively high in kidney tissues. This might be the reason that we only recovered them in the CDK5 purification in HEK293T cells, an embryonic kidney cell line, but not in MCF10A cells, which are normal breast epithelial cells. Another difference is that MCF10A is a normal breast epithelial cell line, its cell cycle regulation could be different from that of HEK293T cells, which express SV40 T antigen. For example, CDK2 binds to CCNA1/2, CCNH, CCNJ only in HEK293T cells, and CCND1/3 only in MCF10A cells
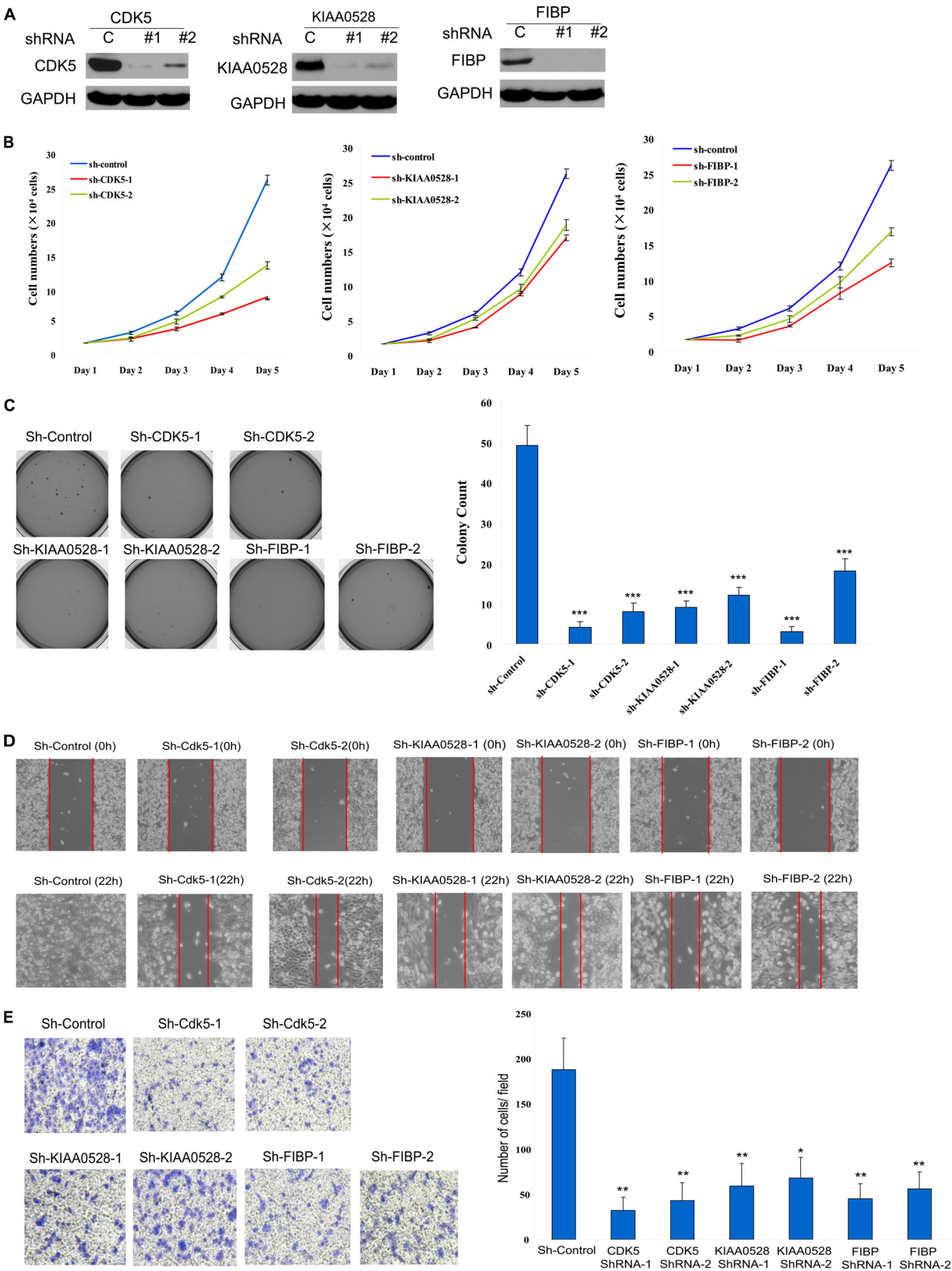
FIG. 6. **CDK5, KIAA0528, and FIBP complex participates in cell growth and migration in breast cancer cells.** *A*, Establishment of two CDK5, KIAA0528, or FIBP knockdown cell lines. Two lentiviral shRNAs for each gene were used to infect MDA-MB-231 cells, and stable knockdown pools were generated with puromycin selection. Cells were harvested and cell lysates were blotted with indicated antibodies.
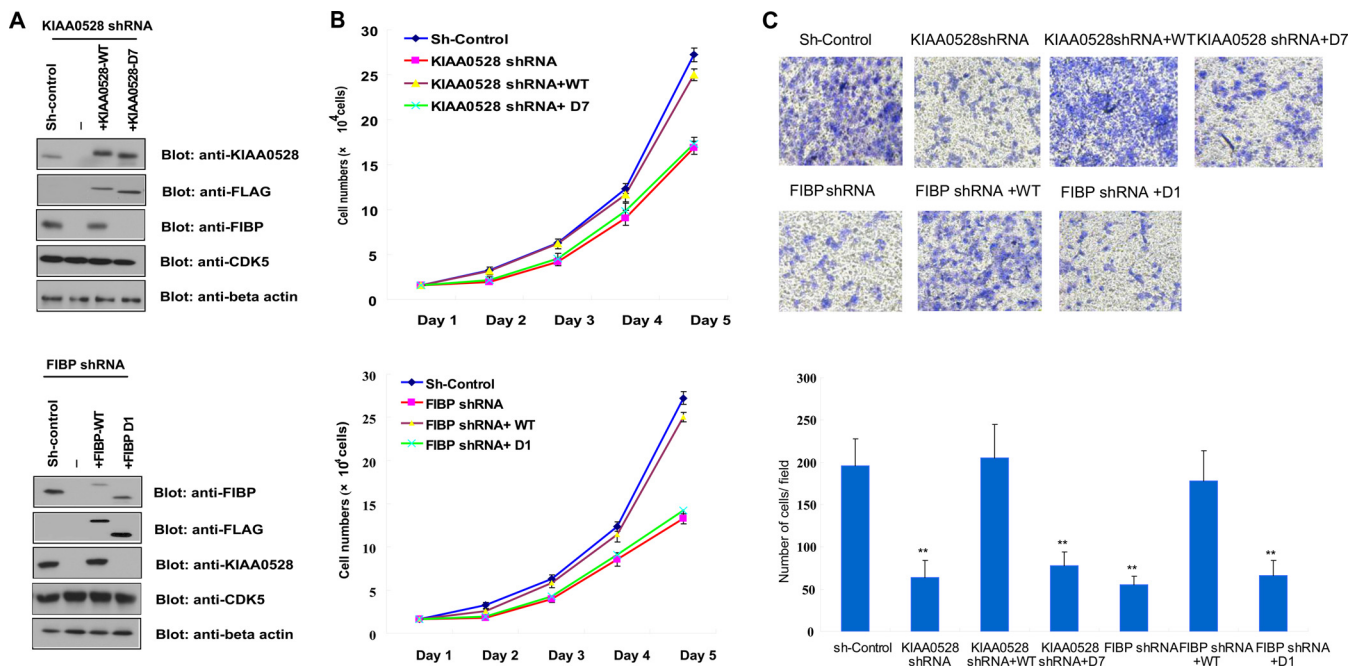
FIG. 7. **Interaction between KIAA0528 and FIBP is required for cell growth and migration in breast cancer cells.** *A*, Restoring wild-type but not the binding deficient mutant of KIAA0528 (or FIBP) expression rescued the decreased level of FIBP (or KIAA0528). KIAA0528 (or FIBP) stable knockdown cells were reconstituted with either wild-type KIAA0528 (or FIBP) or binding deficient mutant as indicated. *B*, Wild-type but not the binding deficient mutant of KIAA0528 (or FIBP) rescued retarded cell proliferation. *C*, Wild-type but not the binding deficient mutant of KIAA0528 (or FIBP) rescued the decreased cell migration *in vitro*. ** $p < 0.01$ compared with controls cells.

(Fig. 3*C*). It is possible that this difference could be caused by the inactivation of both p53 and RB pathways by SV40 T antigen in HEK293T cells, while these cell cycle regulatory pathways are intact in MCF10A cells. Future studies will be needed to elucidate the mechanisms underlying the difference of CDK interactomes in these two cell lines.

More specifically, we identified a novel complex containing CDK5, KIAA0528, and FIBP, and demonstrated that FIBP and KIAA0528 are required for the complex assembly and stability. Importantly, CDK5-, KIAA0528-, or FIBP-depleted breast cancer cells displayed impaired cell growth and decreased cell migration. Given that CDK5 has already been proposed to act in these processes, it is not surprising that KIAA0528 and FIBP are also required for these functions.

Cyclin-dependent kinase 5 (CDK5) is a unique member of the CDK family (9). CDK5 is best known as a neuron-specific kinase, which is largely because of the fact that CDK5 activators p35 and p39 are present only in neuronal cells. Of course, CDK5 also can binds to cyclins, such as cyclin D1/D3/E, but binding to these cyclins does not seem to affect its kinase activity (60, 61). However, cyclin I can bind to and

activate Cdk5 (53), which may be involved in antiapoptotic process via the MAPK signaling pathway. Cyclin E has also been shown to form complexes with Cdk5 and controls synapse function by restraining Cdk5 activity in postmitotic neurons (62). In agreement with these prior publications, we identified cyclin I and other known CDK5 binding partners, such as CABLES1, CABLES2, and CCND2 as CDK5-interacting proteins (Fig. 4*A*), which is consistent with findings from previous reports. Importantly, we identified KIAA0528 and FIBP as the major CDK5-associated proteins in three independent cell lines, indicating that these three proteins form a stable complex in non-neuronal cells. Indeed, a recent high-throughput AP-MS study of 32 human kinases including CDK5 also revealed that KIAA0528 and FIBP are CDK5-interacting proteins (63). Therefore, it is likely that this CDK5/KIAA0528/FIBP complex may play crucial roles in various cellular processes because of its presence in multiple non-neuronal cell lines.

Although many researchers focus on CDK5 functions in neuronal development, increasing evidence is supporting extra-neuronal roles of CDK5, especially in tumorigenesis (12, 17–19). CDK5 was reported to be active and control cell

B, Knockdown of CDK5, KIAA0528, or FIBP impairs cell proliferation. Control transfected cells, CDK5-, KIAA0528-, or FIBP-depleted cells were seeded at low density, and cell proliferation was measured every day by determining the cell numbers. *C*, Colony formation in soft agar is significantly reduced in CDK5-, KIAA0528-, or FIBP-depleted MDA-MB-231 cells. *** $p < 0.001$ compared with controls cells. *D*, Cell migration capability is decreased in CDK5, KIAA0528, or FIBP knockdown cells as determined by wound healing assay. *E*, Cells depleted of CDK5, KIAA0528, or FIBP show decreased cell migration as assessed by the Transwell assay, described in the text. * $p < 0.05$; ** $p < 0.01$ compared with controls cells.

growth and metastasis in prostate and pancreatic cancers (16, 23). CDK5 was also shown to promote prostate cancer cell growth through androgen receptor (24). Cdk5-mediated phosphorylation of PIKE-A was proposed to induce glioblastoma cell migration and invasion (64). Moreover, Cdk5 inhibition led to retarded cell growth in medullary thyroid carcinoma cells, accompanied by reduced phospho-STAT3 (65). In agreement with these studies, we demonstrated that CDK5 and its two major binding partners, KIAA0528 and FIBP, are required for breast cancer cell growth and migration, highlighting that this major CDK5-containing protein complex is likely responsible for most, if not all, of the CDK5 functions in non-neuronal cells. Our future studies will focus on elucidating the mechanism of this complex and how it may regulate multiple cellular processes and contribute to tumorigenesis by promoting tumor proliferation and migration.

In conclusion, our proteomic study of the CDK kinase family led us to establish the first CDK interactomes, which will greatly facilitate future studies of this family of kinases, not only in cell cycle regulations, but also in many other cellular processes. More specifically, involvement of the CDK5 complex in the growth and migration of breast cancer cells suggests that CDK5 may be a promising therapeutic target for cancer therapy, especially for those breast cancers with high levels of CDK5, KIAA0528, and/or FIBP expression.

REFERENCES

1. Morgan, D. O. (1997) Cyclin-dependent kinases: engines, clocks, and microprocessors. *Annu. Rev. Cell Dev. Biol.* **13,** 261–291
2. Malumbres, M., and Barbacid, M. (2005) Mammalian cyclin-dependent kinases. *Trends Biochem. Sci.* **30,** 630–641
3. Satyanarayana, A., and Kaldis, P. (2009) Mammalian cell-cycle regulation: several Cdks, numerous cyclins and diverse compensatory mechanisms. *Oncogene* **28,** 2925–2939
4. Malumbres, M., and Barbacid, M. (2009) Cell cycle, CDKs and cancer: a changing paradigm. *Nat. Rev. Cancer* **9,** 153–166
5. Johnson, N., and Shapiro, G. I. (2010) Cyclin-dependent kinases (cdks) and the DNA damage response: rationale for cdk inhibitor-chemotherapy combinations as an anticancer strategy for solid tumors. *Expert Opin. Ther. Targets.* **14,** 1199–1212
6. Malumbres, M., Harlow, E., Hunt, T., Hunter, T., Lahti, J. M., Manning, G., Morgan, D. O., Tsai, L. H., and Wolgemuth, D. J. (2009) Cyclin-dependent kinases: a family portrait. *Nat. Cell Biol.* **11,** 1275–1276
7. Malumbres, M., and Barbacid, M. (2007) Cell cycle kinases in cancer. *Curr. Opin. Genet. Dev.* **17,** 60–65
8. Malumbres, M. (2011) Physiological relevance of cell cycle kinases. *Physiol. Rev.* **91,** 973–1007
9. Dhariwala, F. A., and Rajadhyaksha, M. S. (2008) An unusual member of the Cdk family: Cdk5. *Cell. Mol. Neurobiol.* **28,** 351–369
10. Tsai, L. H., Delalle, I., Caviness, V. S., Jr., Chae, T., and Harlow, E. (1994) p35 is a neural-specific regulatory subunit of cyclin-dependent kinase 5. *Nature* **371,** 419–423
11. Lew, J., Huang, Q. Q., Qi, Z., Winkfein, R. J., Aebersold, R., Hunt, T., and Wang, J. H. (1994) A brain-specific activator of cyclin-dependent kinase 5. *Nature* **371,** 423–426
12. Contreras-Vallejos, E., Utreras, E., and Gonzalez-Billault, C. (2012) Going out of the brain: non-nervous system physiological and pathological functions of Cdk5. *Cell Signal.* **24,** 44–52
13. Lopes, J. P., and Agostinho, P. (2011) Cdk5: multitasking between physiological and pathological conditions. *Prog. Neurobiol.* **94,** 49–63
14. Lalioti, V., Pulido, D., and Sandoval, I. V. (2010) Cdk5, the multifunctional surveyor. *Cell Cycle* **9,** 284–311
15. Su, S. C., and Tsai, L. H. (2011) Cyclin-dependent kinases in brain development and disease. *Annu. Rev. Cell Dev. Biol.* **27,** 465–491
16. Feldmann, G., Mishra, A., Hong, S. M., Bisht, S., Strock, C. J., Ball, D. W., Goggins, M., Maitra, A., and Nelkin, B. D. (2010) Inhibiting the cyclin-dependent kinase CDK5 blocks pancreatic cancer formation and progression through the suppression of Ras-Ral signaling. *Cancer Res.* **70,** 4460–4469
17. Rosales, J. L., and Lee, K. Y. (2006) Extraneuronal roles of cyclin-dependent kinase 5. *Bioessays* **28,** 1023–1034
18. Liebl, J., Furst, R., Vollmar, A. M., and Zahler, S. (2011) Twice switched at birth: cell cycle-independent roles of the "neuron-specific" cyclin-dependent kinase 5 (Cdk5) in non-neuronal cells. *Cell Signal.* **23,** 1698–1707
19. Arif, A. (2012) Extraneuronal activities and regulatory mechanisms of the atypical cyclin-dependent kinase Cdk5. *Biochem. Pharmacol.* **84,** 985–993
20. Selvendiran, K., Koga, H., Ueno, T., Yoshida, T., Maeyama, M., Torimura, T., Yano, H., Kojiro, M., and Sata, M. (2006) Luteolin promotes degradation in signal transducer and activator of transcription 3 in human hepatoma cells: an implication for the antitumor potential of flavonoids. *Cancer Res.* **66,** 4826–4834
21. Kim, E., Chen, F., Wang, C. C., and Harrison, L. E. (2006) CDK5 is a novel regulatory protein in PPARgamma ligand-induced antiproliferation. *Int. J. Oncol.* **28,** 191–194
22. Eggers, J. P., Grandgenett, P. M., Collisson, E. C., Lewallen, M. E., Tremayne, J., Singh, P. K., Swanson, B. J., Andersen, J. M., Caffrey, T. C., High, R. R., Ouellette, M., and Hollingsworth, M. A. (2011) Cyclin-dependent kinase 5 is amplified and overexpressed in pancreatic cancer and activated by mutant K-Ras. *Clin. Cancer Res.* **17,** 6140–6150
23. Strock, C. J., Park, J. I., Nakakura, E. K., Bova, G. S., Isaacs, J. T., Ball, D. W., and Nelkin, B. D. (2006) Cyclin-dependent kinase 5 activity controls cell motility and metastatic potential of prostate cancer cells. *Cancer Res.* **66,** 7509–7515
24. Hsu, F. N., Chen, M. C., Chiang, M. C., Lin, E., Lee, Y. T., Huang, P. H., Lee, G. S., and Lin, H. (2011) Regulation of androgen receptor and prostate cancer growth by cyclin-dependent kinase 5. *J. Biol. Chem.* **286,** 33141–33149
25. Choi, H. S., Lee, Y., Park, K. H., Sung, J. S., Lee, J. E., Shin, E. S., Ryu, J. S., and Kim, Y. H. (2009) Single-nucleotide polymorphisms in the promoter of the CDK5 gene and lung cancer risk in a Korean population. *J. Hum.*

Genet. **54,** 298–303

26. Lockwood, W. W., Chari, R., Coe, B. P., Girard, L., Macaulay, C., Lam, S., Gazdar, A. F., Minna, J. D., and Lam, W. L. (2008) DNA amplification is a ubiquitous mechanism of oncogene activation in lung and other cancers. *Oncogene* **27,** 4615–4624

27. Shevchenko, A., Wilm, M., Vorm, O., and Mann, M. (1996) Mass spectrometric sequencing of proteins silver-stained polyacrylamide gels. *Anal. Chem.* **68,** 850–858

28. Elias, J. E., and Gygi, S. P. (2007) Target-decoy search strategy for increased confidence in large-scale protein identifications by mass spectrometry. *Nat. Methods* **4,** 207–214

29. Vizcaino, J. A., Cote, R. G., Csordas, A., Dianes, J. A., Fabregat, A., Foster, J. M., Griss, J., Alpi, E., Birim, M., Contell, J., O'Kelly, G., Schoenegger, A., Ovelleiro, D., Perez-Riverol, Y., Reisinger, F., Rios, D., Wang, R., and Hermjakob, H. (2013) The PRoteomics IDEntifications (PRIDE) database and associated tools: status in 2013. *Nucleic Acids Res.* **41,** D1063–D1069

30. Vizcaino, J. A., Deutsch, E. W., Wang, R., Csordas, A., Reisinger, F., Rios, D., Dianes, J. A., Sun, Z., Farrah, T., Bandeira, N., Binz, P. A., Xenarios, I., Eisenacher, M., Mayer, G., Gatto, L., Campos, A., Chalkley, R. J., Kraus, H. J., Albar, J. P., Martinez-Bartolome, S., Apweiler, R., Omenn, G. S., Martens, L., Jones, A. R., and Hermjakob, H. (2014) Proteome-Xchange provides globally coordinated proteomics data submission and dissemination. *Nat. Biotechnol.* **32,** 223–226

31. Cote, R. G., Griss, J., Dianes, J. A., Wang, R., Wright, J. C., van den Toorn, H. W., van Breukelen, B., Heck, A. J., Hulstaert, N., Martens, L., Reisinger, F., Csordas, A., Ovelleiro, D., Perez-Riverol, Y., Barsnes, H., Hermjakob, H., and Vizcaino, J. A. (2012) The PRoteomics IDEntification (PRIDE) Converter 2 framework: an improved suite of tools to facilitate data submission to the PRIDE database and the ProteomeXchange consortium. *Mol. Cell. Proteomics* **11,** 1682–1689

32. Choi, H., Larsen, B., Lin, Z. Y., Breitkreutz, A., Mellacheruvu, D., Fermin, D., Qin, Z. S., Tyers, M., Gingras, A. C., and Nesvizhskii, A. I. (2011) SAINT: probabilistic scoring of affinity purification-mass spectrometry data. *Nat. Methods* **8,** 70–73

33. Saito, R., Smoot, M. E., Ono, K., Ruscheinski, J., Wang, P. L., Lotia, S., Pico, A. R., Bader, G. D., and Ideker, T. (2012) A travel guide to Cytoscape plugins. *Nat. Methods* **9,** 1069–1076

34. Smoot, M. E., Ono, K., Ruscheinski, J., Wang, P. L., and Ideker, T. (2011) Cytoscape 2.8: new features for data integration and network visualization. *Bioinformatics* **27,** 431–432

35. Chatr-Aryamontri, A., Breitkreutz, B. J., Heinicke, S., Boucher, L., Winter, A., Stark, C., Nixon, J., Ramage, L., Kolas, N., O'Donnell, L., Reguly, T., Breitkreutz, A., Sellam, A., Chen, D., Chang, C., Rust, J., Livstone, M., Oughtred, R., Dolinski, K., and Tyers, M. (2013) The BioGRID interaction database: 2013 update. *Nucleic Acids Res.* **41,** D816–D823

36. Wang, J., Leung, J. W., Gong, Z., Feng, L., Shi, X., and Chen, J. (2013) PHF6 regulates cell cycle progression by suppressing ribosomal RNA synthesis. *J. Biol. Chem.* **288,** 3174–3183

37. Wang, W., Huang, J., Wang, X., Yuan, J., Li, X., Feng, L., Park, J. I., and Chen, J. (2012) PTPN14 is required for the density-dependent control of YAP1. *Genes Dev.* **26,** 1959–1971

38. Wang, W., Huang, J., and Chen, J. (2011) Angiomotin-like proteins associate with and negatively regulate YAP1. *J. Biol. Chem.* **286,** 4364–4370

39. Chen, D., Sun, Y., Wei, Y., Zhang, P., Rezaeian, A. H., Teruya-Feldstein, J., Gupta, S., Liang, H., Lin, H. K., Hung, M. C., and Ma, L. (2012) LIFR is a breast cancer metastasis suppressor upstream of the Hippo-YAP pathway and a prognostic marker. *Nat. Med.* **18,** 1511–1517

40. Choi, H., Larsen, B., Lin, Z. Y., Breitkreutz, A., Mellacheruvu, D., Fermin, D., Qin, Z. S., Tyers, M., Gingras, A. C., and Nesvizhskii, A. I. (2011) SAINT: probabilistic scoring of affinity purification-mass spectrometry data. *Nat. Methods* **8,** 70–73

41. Breitkreutz, A., Choi, H., Sharom, J. R., Boucher, L., Neduva, V., Larsen, B., Lin, Z. Y., Breitkreutz, B. J., Stark, C., Liu, G., Ahn, J., Dewar-Darch, D., Reguly, T., Tang, X., Almeida, R., Qin, Z. S., Pawson, T., Gingras, A. C., Nesvizhskii, A. I., and Tyers, M. (2010) A global protein kinase and phosphatase interaction network in yeast. *Science* **328,** 1043–1046

42. Wang, W., Li, X., Huang, J., Feng, L., Dolinta, K. G., and Chen, J. (2014) Defining the protein-protein interaction network of the human Hippo pathway. *Mol. Cell. Proteomics* **13,** 119–131

43. Mellacheruvu, D., Wright, Z., Couzens, A. L., Lambert, J. P., St-Denis, N. A., Li, T., Miteva, Y. V., Hauri, S., Sardiu, M. E., Low, T. Y., Halim, V. A., Bagshaw, R. D., Hubner, N. C., Al-Hakim, A., Bouchard, A., Faubert, D., Fermin, D., Dunham, W. H., Goudreault, M., Lin, Z. Y., Badillo, B. G., Pawson, T., Durocher, D., Coulombe, B., Aebersold, R., Superti-Furga, G., Colinge, J., Heck, A. J., Choi, H., Gstaiger, M., Mohammed, S., Cristea, I. M., Bennett, K. L., Washburn, M. P., Raught, B., Ewing, R. M., Gingras, A. C., and Nesvizhskii, A. I. (2013) The CRAPome: a contaminant repository for affinity purification-mass spectrometry data. *Nat. Methods* **10,** 730–736

44. Choi, H., Fermin, D., and Nesvizhskii, A. I. (2008) Significance analysis of spectral count data in label-free shotgun proteomics. *Mol. Cell. Proteomics* **7,** 2373–2385

45. Sato, S., Tomomori-Sato, C., Parmely, T. J., Florens, L., Zybailov, B., Swanson, S. K., Banks, C. A., Jin, J., Cai, Y., Washburn, M. P., Conaway, J. W., and Conaway, R. C. (2004) A set of consensus mammalian mediator subunits identified by multidimensional protein identification technology. *Mol. Cell* **14,** 685–691

46. Chen, H. H., Wang, Y. C., and Fann, M. J. (2006) Identification and characterization of the CDK12/cyclin L1 complex involved in alternative splicing regulation. *Mol. Cell. Biol.* **26,** 2736–2745

47. Chen, H. H., Wong, Y. H., Geneviere, A. M., and Fann, M. J. (2007) CDK13/CDC2L5 interacts with L-type cyclins and regulates alternative splicing. *Biochem. Biophys. Res. Commun.* **354,** 735–740

48. Zolotukhin, A. S., Uranishi, H., Lindtner, S., Bear, J., Pavlakis, G. N., and Felber, B. K. (2009) Nuclear export factor RBM15 facilitates the access of DBP5 to mRNA. *Nucleic Acids Res.* **37,** 7151–7162

49. Zhou, A., Ou, A. C., Cho, A., Benz, E. J., Jr., and Huang, S. C. (2008) Novel splicing factor RBM25 modulates Bcl-x pre-mRNA 5′ splice site selection. *Mol. Cell. Biol.* **28,** 5924–5936

50. Zukerberg, L. R., Patrick, G. N., Nikolic, M., Humbert, S., Wu, C. L., Lanier, L. M., Gertler, F. B., Vidal, M., Van Etten, R. A., and Tsai, L. H. (2000) Cables links Cdk5 and c-Abl and facilitates Cdk5 tyrosine phosphorylation, kinase upregulation, and neurite outgrowth. *Neuron* **26,** 633–646

51. Sato, H., Nishimoto, I., and Matsuoka, M. (2002) ik3–2, a relative to ik3–1/cables, is associated with cdk3, cdk5, and c-abl. *Biochim. Biophys. Acta* **1574,** 157–163

52. Guidato, S., McLoughlin, D. M., Grierson, A. J., and Miller, C. C. (1998) Cyclin D2 interacts with cdk-5 and modulates cellular cdk-5/p35 activity. *J. Neurochem.* **70,** 335–340

53. Brinkkoetter, P. T., Olivier, P., Wu, J. S., Henderson, S., Krofft, R. D., Pippin, J. W., Hockenbery, D., Roberts, J. M., and Shankland, S. J. (2009) Cyclin I activates Cdk5 and regulates expression of Bcl-2 and Bcl-XL in post-mitotic mouse cells. *J. Clin. Invest.* **119,** 3089–3101

54. Xie, X., Gong, Z., Mansuy-Aubert, V., Zhou, Q. L., Tatulian, S. A., Sehrt, D., Gnad, F., Brill, L. M., Motamedchaboki, K., Chen, Y., Czech, M. P., Mann, M., Kruger, M., and Jiang, Z. Y. (2011) C2 domain-containing phospho-protein CDP138 regulates GLUT4 insertion into the plasma membrane. *Cell Metab.* **14,** 378–389

55. Sadacca, L. A., Bruno, J., Wen, J., Xiong, W., and McGraw, T. E. (2013) Specialized sorting of GLUT4 and its recruitment to the cell surface are independently regulated by distinct Rabs. *Mol. Biol. Cell* **24,** 2544–2557

56. Kolpakova, E., Wiedlocha, A., Stenmark, H., Klingenberg, O., Falnes, P. O., and Olsnes, S. (1998) Cloning of an intracellular protein that binds selectively to mitogenic acidic fibroblast growth factor. *Biochem. J.* **336,** 213–222

57. Kolpakova, E., Frengen, E., Stokke, T., and Olsnes, S. (2000) Organization, chromosomal localization and promoter analysis of the gene encoding human acidic fibroblast growth factor intracellular binding protein. *Biochem. J.* **352,** 629–635

58. Forde, N., Mihm, M., Canty, M. J., Zielak, A. E., Baker, P. J., Park, S., Lonergan, P., Smith, G. W., Coussens, P. M., Ireland, J. J., and Evans, A. C. (2008) Differential expression of signal transduction factors in ovarian follicle development: a functional role for betaglycan and FIBP in granulosa cells in cattle. *Physiol. Genomics* **33,** 193–204

59. Yin, J., Sobeck, A., Xu, C., Meetei, A. R., Hoatlin, M., Li, L., and Wang, W. (2005) BLAP75, an essential component of Bloom's syndrome protein complexes that maintain genome integrity. *EMBO J.* **24,** 1465–1476

60. Xiong, Y., Zhang, H., and Beach, D. (1992) D type cyclins associate with multiple protein kinases and the DNA replication and repair factor PCNA. *Cell* **71,** 505–514

61. Miyajima, M., Nornes, H. O., and Neuman, T. (1995) Cyclin E is expressed in neurons and forms complexes with cdk5. *Neuroreport* **6,** 1130–1132

62. Odajima, J., Wills, Z. P., Ndassa, Y. M., Terunuma, M., Kretschmannova, K., Deeb, T. Z., Geng, Y., Gawrzak, S., Quadros, I. M., Newman, J., Das, M., Jecrois, M. E., Yu, Q., Li, N., Bienvenu, F., Moss, S. J., Greenberg, M. E., Marto, J. A., and Sicinski, P. (2011) Cyclin E constrains Cdk5 activity to regulate synaptic plasticity and memory formation. *Dev. Cell* **21,** 655–668

63. Varjosalo, M., Sacco, R., Stukalov, A., van Drogen, A., Planyavsky, M., Hauri, S., Aebersold, R., Bennett, K. L., Colinge, J., Gstaiger, M., and Superti-Furga, G. (2013) Interlaboratory reproducibility of large-scale human protein-complex analysis by standardized AP-MS. *Nat. Methods* **10,** 307–314

64. Liu, R., Tian, B., Gearing, M., Hunter, S., Ye, K., and Mao, Z. (2008) Cdk5-mediated regulation of the PIKE-A-Akt pathway and glioblastoma cell invasion. *Proc. Natl. Acad. Sci. U. S. A.* **105,** 7570–7575

65. Lin, H., Chen, M. C., Chiu, C. Y., Song, Y. M., and Lin, S. Y. (2007) Cdk5 regulates STAT3 activation and cell proliferation in medullary thyroid carcinoma cells. *J. Biol. Chem.* **282,** 2776–2784